

The mechanism of anticancer effects of some pyrrolopyrimidine derivatives on HT-29 human colon cancer cells

Mustafa Ergul^a, Zuhail Kilic-Kurt^{b,*}, Yeliz Aka^c, Ozgur Kutuk^c, Zeynep Deniz Sahin-Inan^d

^a Department of Biochemistry, Faculty of Pharmacy, Sivas Cumhuriyet University, Sivas, Turkey

^b Department of Pharmaceutical Chemistry, Faculty of Pharmacy, Ankara University, Ankara, Turkey

^c Baskent University School of Medicine, Department of Immunology, Adana Dr. Turgut Noyan Medical and Research Center, Adana, Turkey

^d Department of Histology and Embryology, Faculty of Medicine, Sivas Cumhuriyet University, Sivas, Turkey

ARTICLE INFO

Editor: Dr. J Davila

Keywords:

Apoptosis
Cell cycle
Cytotoxicity
ELISA
Immunohistochemistry
Pyrrolopyrimidines

ABSTRACT

In the present work, the mechanism of anticancer activity of some pyrrolopyrimidine derivatives was evaluated. Compounds **5** and **8** exhibiting significant antiproliferative activity against HT-29 cells with IC₅₀ values of 4.17 μM and 2.96, arrested the cells at the G2/M phase and significantly induced apoptosis. The apoptotic potential of the compounds has been verified via ELISA assay, which resulted in increased BAX, PUMA, BIM, and cleaved caspase 3 expression and decreased BCL-XL and MCL-1 protein levels in HT-29 cells. Moreover, the immunofluorescence technique showing that compounds **5** and **8**-treatment reduced Ki67 immunolocalization and increased the caspase 3 and p53 immunolocalization confirmed the apoptotic activity. While treatment of HT-29 cells to compounds **5** and **8** inhibited Akt and ERK1/2, there are no alterations in JNK and p38 signaling pathways. According to molecular docking results, compounds **5** and **8** occupied the active site of Akt kinase and showed important hydrogen bonding interactions with key amino acids. Also, siRNA-mediated depletion of BIM, PUMA, and BAX/BAK expression decreased apoptotic response in HT-29 cells upon exposure to compound **5** and compound **8**. Compounds **5** and **8** trigger the activation of mitochondrial apoptosis in HT-29 cells. Additionally, we found that proapoptotic BH3-only proteins BIM and PUMA are required for the full engagement of mitochondrial apoptosis signaling. However, p53 was dispensable for compound **5**- or compound **8**-induced apoptosis in HT-29 cells.

1. Introduction

Cancer has been linked to the overexpression of signaling that regulates normal cell growth, differentiation, motility, and adhesion (Chen and Fu, 2011). Apoptosis assumes a pivotal function in regulating these physiological cellular processes. It has been shown that therapy resistance in various cancers is mediated by dysregulation in the mitochondrial apoptotic system (Fulda and Debatin, 2004). Members of the BCL-2 protein family control mitochondrial apoptosis signaling. BCL-2 proteins primarily control the permeabilization of the mitochondrial outer membrane (MOMP) and the release of cytochrome *c* into the cytoplasm (Singh et al., 2019). We and others have shown that the inhibition of intrinsic apoptotic signaling leads to resistance against conventional and targeted chemotherapy (Kutuk and Letai, 2008; De Graaff et al., 2016; Johnson-Farley et al., 2015; Oakes et al., 2012). p53 is a critical protein for intrinsic tumor suppression through cell cycle arrest and promoting

apoptosis. Some chemotherapy drugs affect cancer cells by leading to apoptotic death via a p53-dependent pathway (Indran et al., 2011). DNA damage and oncogene activation can also trigger the activation of p53. The activation of p53 increases the levels of several proapoptotic proteins (Bax, PUMA, Noxa, and Bid) and suppresses antiapoptotic proteins (Bcl-2, Bcl-X_L, and surviving). The induction of pro-apoptotic proteins causes mitochondria to release cytochrome *c*, which triggers caspase activation, including caspase 3 (Elmore, 2007; Reed, 2000; Testa and Riccioni, 2007). Apoptosis has also been affected by exogenous reactive oxygen species (ROS) or ROS-inducing agents that upregulate some death receptors such as CD95, and TRAIL, and cause DNA damage. ROS appears to be responsible for later mitochondrial events and leads to full activation of the caspases and, finally apoptosis (Jeong and Joo, 2016; Simon et al., 2000). The development of novel agents that can trigger apoptotic death through several mechanisms is an essential approach to cancer treatment. Despite notable progress in the field of cancer biology

* Corresponding author.

E-mail address: zkurt@ankara.edu.tr (Z. Kilic-Kurt).

<https://doi.org/10.1016/j.tiv.2023.105757>

Received 1 August 2023; Accepted 30 November 2023

Available online 5 December 2023

0887-2333/© 2023 Elsevier Ltd. All rights reserved.

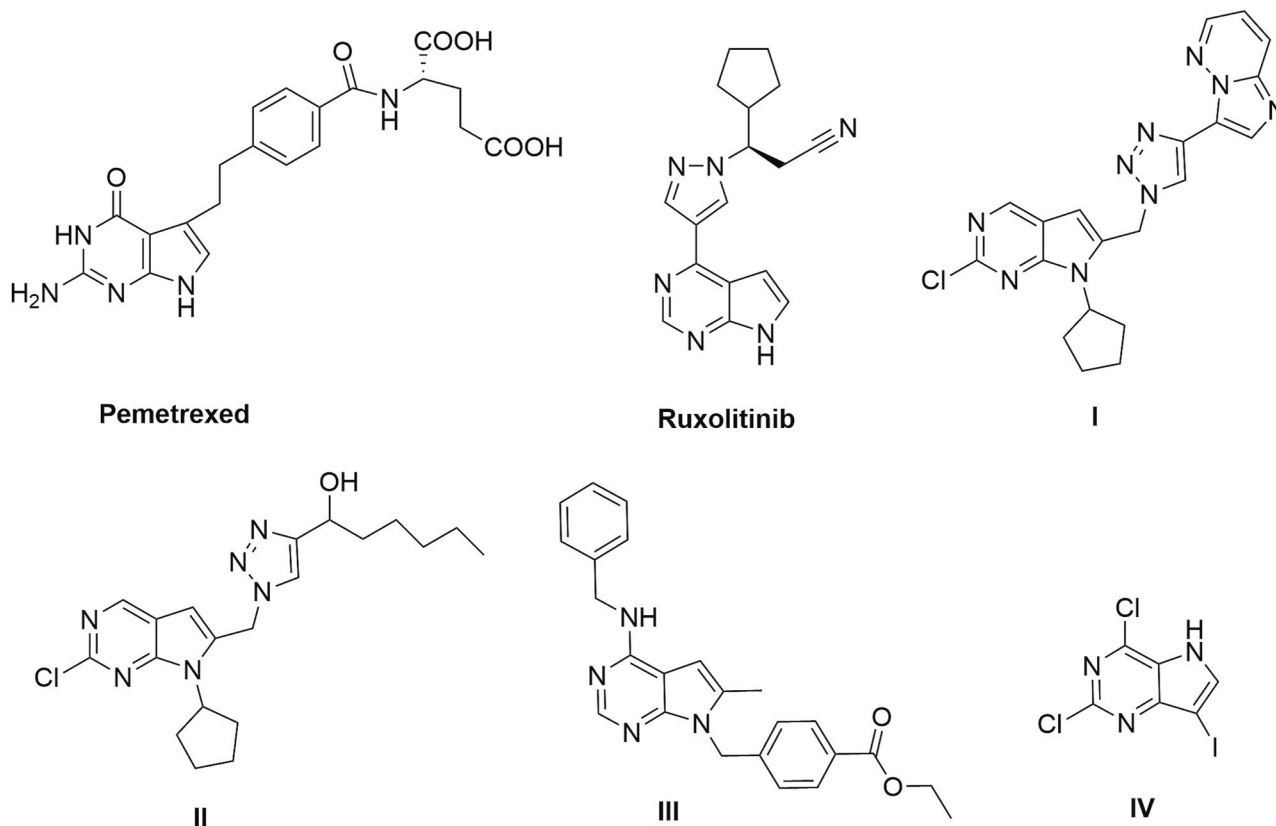


Fig. 1. Pyrrolopyrimidine-based compounds having anticancer activities.

and treatment strategies, the development of novel drugs providing a safety profile with less toxicity and high efficiency is urgently needed.

Pyrrolopyrimidine is a beneficial scaffold due to its analogous nature to purine nucleosides and its diverse activities (Pathania and Rawal, 2018). Currently, a number of the FDA-approved drugs bearing pyrrolopyrimidine scaffold are used or in clinical trials for cancer management. Antifolate **Pemetrexed** (Fig. 1) is one of the most commonly used drugs to treat nonsquamous NSCLC (Goldman and Zhao, 2002; Tomasini et al., 2016). **Ruxolitinib** (Fig. 1), a highly effective and specific oral inhibitor of JAK1 and JAK2, is currently in clinical evaluation for the treatment of ovarian, metastatic breast, and pancreatic malignancies (Yu et al., 2017; Hurwitz et al., 2015). Moreover, the antiproliferative activity of pyrrolopyrimidines have been extensively noted in the literature, and many different mechanisms of action have been presented (Mohamed et al., 2017; De Coen et al., 2016). Thiriveedhi et al. reported some pyrrolopyrimidine derivatives bearing triazole moiety and their anticancer activity on melanoma and breast cancer cell lines. In that study, compounds substituted with imidazo[1,2-*b*]pyridazin (I) and hexanol group (II) exhibited anti-proliferative activity against both cancer cells in the micromolar range (Thiriveedhi et al., 2019). Gilson et al. identified a new pyrrolopyrimidine compound that strongly induced apoptosis and mitotic cell blockade by high throughput cell-based screening. Compound III has demonstrated efficacy against resistant cell lines with no remarkable toxicity to the chicken embryo in vivo (Gilson et al., 2017). Temburnikar et al. reported halogenated pyrrolo[3,2-*d*]pyrimidine derivatives and their antiproliferative activities against various cancer cell lines. Among them, compound IV showed significant anticancer activity against breast cancer cells through cell cycle arrest at the G2/M phase (Temburnikar et al., 2015).

In the present study, the mechanism of anticancer activity of previously synthesized (Kilic-Kurt et al., 2019; Kilic-Kurt et al., 2018) pyrrolopyrimidine-based target compounds was evaluated. Firstly, we tested the antiproliferative activity of compounds against MDA-MB-231,

C6, and HT-29 cancer cell lines, and noncancerous L929 cells. Then, compounds 5 and 8 were selected to explore the mechanism of the activity, since they showed the highest cytotoxicity in HT-29 cells. The effects of compounds 5 and 8 on prosurvival signaling pathways and mitochondrial apoptosis in HT-29 cells were evaluated. Besides, to support the cytotoxic and apoptotic effects of compounds 5 and 8, total oxidant status (TOS) was determined in the compounds 5, 8-treated, and -untreated HT-29 cells. To predict the binding mode of compounds with the Akt kinase, a molecular docking study was performed.

2. Materials and methods

2.1. Cell culture conditions and reagents

MDA-MB-231 (HTB-26), C6 (CCL-107), HT-29 (HTB-38), and L929 (CRL-6364) cells were obtained from American Type Culture Collection (Manassas, VA, USA) and maintained in Dulbecco's Modified Eagle's Medium (DMEM) (Sigma- Aldrich) supplemented with 10% (v/v) heat-inactivated FBS (Gibco, Thermo Fisher Scientific) and 1% penicillin/streptomycin (Gibco, Thermo Fisher Scientific). The cells were cultured in a 25 cm² cell culture flask and incubated at 37 °C in a 5% CO₂ humidified atmosphere until they reached approximately 80% confluence. The positive control used in the study was cisplatin (Sigma-Aldrich).

2.2. Cell viability assay

The antiproliferative activities of the target compounds and cisplatin were measured via XTT (2,3-bis-(2-methoxy-4-nitro-5-sulphophenyl)-2H-tetrazolium-5-carboxanilide) colorimetric assay (Roche Diagnostic, Germany). Cancer or normal cells (1×10^4 cells/mL) were seeded in 96-well plates in a 100- μ L culture medium and incubated overnight before treatment. The compounds and cisplatin were dissolved in cell culture grade dimethyl sulfoxide (DMSO concentration did not exceed 0.1%)

and diluted in DMEM before treatment. To screen antiproliferative activities of the compounds (1–14), the cancer cells were firstly treated with 10- μ M constant concentrations of compounds or vehicle (0.1% DMSO) for 24 h. To determine the IC₅₀ values of compounds **5** and **8**, which were found as the most potent compounds, HT-29 cells were also treated with compounds **5** and **8** at 0.5, 1, 2, 5, 10, 20, and 40 μ M concentrations for 24 h. Moreover, all the studied cancer cell lines and L929 cells were subjected to cisplatin at 1, 10, 20, 40, 80, and 100 μ M concentrations to calculate the IC₅₀ values of these cell lines for 24 h. Then, the medium was removed and 100 μ L fresh colorless DMEM (Sigma-Aldrich) was added. A 50 μ L XTT labeling mixture was added to each well to determine living cells, and then the plates were maintained at 37 °C for 4 h. After mixing, the absorbance of XTT-formazan was measured at 450 nm through the use of an ELISA microplate reader (Thermo, Germany). All experiments were conducted in three separate trials, and cell viability was indicated as a percentage relative to the control (100% of viability). Using the following formula: $SI = IC_{50}$ for normal cell line / IC_{50} for cancer cell line, the selectivity index (SI) values were also calculated (Ergul and Bakar-Ates, 2019).

2.3. Cell cycle analysis

Muse Cell Cycle Assay Kit (Merck Millipore, Germany) was used to evaluate cell cycle arrest according to the user's guide. For the treatment of HT-29 cells, IC₅₀ concentrations of compounds **5** and **8** were used. An assay was performed as previously reported (Türe et al., 2021).

2.4. Annexin V binding assay

HT-29 cells treated with IC₅₀ concentrations of compounds **5** and **8** for 24 h and using the Muse Annexin V/Dead Cell (Merck Millipore, Germany) and Annexin V-FITC/PI staining kit (BD Biosciences, San Diego, CA, USA) were used for determining the apoptotic effect of compounds, according to the report in our previous study (Ergul and Bakar-Ates, 2019). All experiments were conducted in three separate trials. The colony-forming assay was previously reported in our study (Karakas et al., 2018).

2.5. Measurement of TOS

Quantitative measurements of TOS in the compounds-treated and -untreated HT-29 cells were determined using the Total Oxidant Status Assay Kit (Rel Assay Diagnostics, Gaziantep, Turkey). HT-29 cells were treated with compounds **5** and **8** at the IC₅₀ concentration for 24 h, and the manufacturer's protocol was followed. The results were presented in μ mol H₂O₂ equivalent/L.

2.6. Caspase 3, Ki67, P53 immunofluorescent staining

To Ki67, Caspase 3, and P53 immunofluorescent staining, HT-29 cells were grown in sterile 6-well culture dishes and treated with compounds **5** and **8** at IC₅₀ concentrations for 24 h. After incubation, the wells were washed with phosphate-buffered saline (PBS) (Sigma Aldrich, Germany), and the cells were fixed in pH 7.4% paraformaldehyde (Merk, Germany) for 10 min at room temperature. After fixation, the wells were washed three times with cold PBS. The cells were then left in sodium citrate buffer (pH 6.5) (Sigma Aldrich, Germany) for 10 min at 95 °C to elicit their antigens and then washed twice with PBS. For permeabilization of the cells, they were incubated in 0.1% Triton™ X-100 (Sigma Aldrich, Germany) solution for 10 min and then washed with PBS. After washing, the Ultra V Block (Thermo Scientific, PBQ180830, USA) was dropped and waited at room temperature for 30 min to prevent non-specific binding. Primary antibodies (Rabbit Polyclonal Caspase3 CPP32 (Thermo Scientific, USA), Mouse Monoclonal anti-Ki67, Clone GM010 (Genemed, Germany), Mouse Monoclonal anti-P53, Clone BP-53-12 (Genemed, Germany) were applied to these cells.

The cells were kept in the dark overnight at +4 °C. At the end of the period, the cells were washed twice with PBS. The secondary antibody (Goat Anti-Rabbit IgG H&L (Alexa Fluor® 568) (ab175471) (Abcam, USA) was applied to the cells for one hour at 36 °C in the dark to make anti-Ki67 and anti-P53 primary antibodies visible. On the other hand, a secondary antibody to Goat Anti-Mouse IgG H & L (Alexa Fluor® 488) (ab150113) (Abcam, USA) was used to ensure that the Caspase 3 primary antibody was visible in cells. At the end of the period, the cells were washed twice with PBS. The fluorescent microscopy (Olympus BX51, Japan) was examined using suitable filters for fluorescence examination and then by making a registration. Immunofluorescence intensity scores (IFIS) were also determined according to the report in a previous study (Sena et al., 2018).

2.7. Bax, cleaved caspase 3, and BCL-2 expression analyses

To evaluate the Bax, cleaved caspase 3, and BCL-2 protein expression in the compounds **5** and **8** treated and untreated HT-29 cells, Human Bax ELISA Kit (Abcam, Catalog #ab199080), Caspase 3 (cleaved) Human ELISA Kit (Invitrogen, Catalog # KHO1091), and BCL-2 Human ELISA Kit (Invitrogen, Catalog # BMS244–3) were used, respectively. Shortly, HT-29 cells were seeded in a 6-well plate and treated with the IC₅₀ concentration of compounds **5** and **8** for 24 h. After that, using the lysis buffer inhibitor-treated and untreated HT-29 cells were lysed and Bax, cleaved caspase 3, and BCL-2 levels in the cell lysates were determined according to the manufacturer's guideline. The total protein concentrations in HT-29 cells were determined using the BCA assay (Pierce Biotechnology, Rockford, IL, USA).

2.8. Enzyme-linked immunosorbent assays

Phosphorylation of Akt on S473 (Human/Mouse/Rat Phospho-Akt (S473) Immunoassay, R&D Systems, #KCB887), phosphorylation of Akt on T308 (Human/Mouse/Rat Phospho-Akt (T308) Immunoassay, R&D Systems, #KCB8871), phosphorylation of ERK1/2 on T202/Y204 and T185/Y187 (Human/Mouse/Rat Phospho-ERK1 (T202/Y204)/ERK2 (T185/Y187) Immunoassay, R&D Systems, #KCB1018), phosphorylation of JNK on T183/Y185 (Human/Mouse/Rat Phospho-JNK (T183/Y185) Immunoassay, R&D Systems, #KCB1205) and phosphorylation of p38 on T180/Y182 (Human/Mouse Phospho-p38 MAP Kinase (T180/Y182) Immunoassay, R&D Systems, #KCB869) were evaluated by cell-based ELISA assays as described by the manufacturer. Results were shown as normalized fluorescence units representing mean \pm SEM of three independent experiments in duplex.

2.9. Real-time qPCR

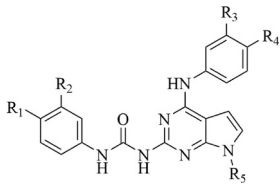
Total RNA was isolated from cells using a RNeasy kit (Qiagen). PCR-based microarrays for evaluating the expression of apoptosis genes were performed using the Human Apoptosis RT² Profiler PCR Array (Qiagen, 330,231, PAHS-012ZA) following manufacturer's instructions. To evaluate mRNA expression of PUMA (BBC3) and NOXA (PMAIP), qRT-PCR was carried out using QuantiTect Primer assays (Hs_BBC3_1_SG QuantiTect Primer Assay, NM_001127240 and Hs_PMAIP1_1_SG, NM_021127; Qiagen) and 1-step QuantiTect SYBR Green qRT-PCR Kit (Qiagen) according to the manufacturer's protocol on LightCycler 480 instrument (Roche). The housekeeping genes on the array were used for normalization and relative gene expression levels were calculated using 2^{- $\Delta\Delta$ CT} method. Data were shown as log₂ expression by using heat-map graphs (Fig. S2). Volcano plots and data tables were provided in Fig. S3. *P*-value < 0.05 and a fold change >3.0 were considered to be significant.

2.10. siRNA transfections

Cells were transfected with BIM siRNA (Hs_BCL2L11_5 FlexiTube siRNA, NM_001204108, Qiagen), PUMA siRNA (Hs_BBC3_2 FlexiTube

Table 1

The percentage cell viability (CV%) of the cancer cell lines after 24 h of exposure to synthesized compounds at 10 μ M.



Cmpd	R ₁	R ₂	R ₃	R ₄	R ₅	CV (% \pm SD)		
						MDA-MB-231	C6	HT-29
1	F	H	H	Cl	CH ₃	83.97 \pm 4.31	96.53 \pm 4.52	61.12 \pm 4.17
2	Cl	CF ₃	Br	H	CH ₃	79.22 \pm 2.02	96.09 \pm 5.42	64.79 \pm 3.42
3	Cl	CF ₃	Cl	F	CH ₃	75.57 \pm 3.22	99.06 \pm 2.79	82.63 \pm 1.97
4	H	CF ₃	Br	H	CH ₃	69.34 \pm 4.11	98.37 \pm 4.86	55.46 \pm 2.57
5	H	CF ₃	Cl	F	CH ₃	58.84 \pm 1.99	92.21 \pm 4.23	23.82 \pm 1.09
6	F	CF ₃	Br	H	CH ₃	50.87 \pm 2.45	91.22 \pm 2.73	36.71 \pm 2.17
7	F	CF ₃	Cl	F	CH ₃	52.84 \pm 2.38	99.15 \pm 4.76	38.37 \pm 2.73
8	H	CF ₃	CF ₃	H	H	40.45 \pm 1.87	83.54 \pm 3.14	21.44 \pm 1.71
9	Cl	CF ₃	Br	H	H	56.75 \pm 2.24	96.11 \pm 4.59	85.66 \pm 3.96
10	Cl	CF ₃	Cl	F	H	49.67 \pm 1.97	91.21 \pm 2.43	61.71 \pm 3.77
11	H	CF ₃	Br	H	H	51.46 \pm 2.57	93.42 \pm 3.17	52.91 \pm 3.74
12	H	CF ₃	H	Cl	H	50.18 \pm 2.86	90.12 \pm 3.24	46.79 \pm 2.23
13	H	CF ₃	H	F	H	51.49 \pm 4.71	85.94 \pm 2.97	32.42 \pm 1.15
14	F	H	Br	H	H	45.54 \pm 3.45	70.02 \pm 3.79	35.82 \pm 1.07

siRNA, Qiagen), BAX (Hs_BAX_8 FlexiTube siRNA, Qiagen), BAK (Hs_BAK1_5 FlexiTube siRNA, Qiagen), p53 (Hs_TP53_9 FlexiTube siRNA, Qiagen) and negative control (scrambled) siRNA (AllStars Negative Control siRNA, Qiagen) by using Hiperfect transfection reagent (Qiagen) according to manufacturer's instructions. The verification of protein knockdown efficiencies through siRNA transfection was conducted by performing immunoblotting 48 h after the transfection process. To conduct 3D cell culture oncospheroid experiments, HT-29 cells were transfected with appropriate siRNA duplex for 24 h, and transferred to an AlgiMatrix 3D culture plate for the growth of cell spheroids in the presence of siRNA treatment every 24 h.

2.11. Immunoprecipitation and immunoblotting

Preparation of total protein lysates and details of immunoprecipitation and immunoblotting were described in our previous study (Temel et al., 2020). Antibodies used for immunoblotting were as follows: MCL-1 (#94296, Cell Signaling), BCL-2 (#2872, Cell Signaling), BCL-X_L (#2762, Cell Signaling), Actin (#8457, Cell Signaling), NOXA (#14766, Cell Signaling), BIM (#2933, Cell Signaling), PUMA (#98672, Cell Signaling), Cytochrome *c* (#4272, Cell Signaling), CoxIV (#4844, Cell Signaling), BAX (#2774, Cell Signaling), BAK (#3814, Cell Signaling), Cleaved Caspase-3 (Asp175) (#9661, Cell Signaling), Cleaved Caspase-9 (Asp315) (#20750, Cell signaling), Cleaved PARP (Asp214) (#5625, Cell Signaling).

2.12. Subcellular fractionation

Subcellular fractionation was performed as described before (Ruiz-Vela et al., 2005). After the indicated treatments, cells were harvested, rinsed with ice-cold PBS, and resuspended in an isotonic buffer [250 mmol/L sucrose, 20 mmol/L HEPES (pH 7.5), 10 mM potassium chloride, 1.5 mM magnesium chloride, 1 mM EDTA, 1 mM EGTA, 1 mM PMSF, and protease inhibitors [cComplete ULTRA, Roche] on ice during 20 min. After incubation, the cells were homogenized using a Dounce homogenizer and centrifuged for 10 min at 800g and 4 °C. To obtain mitochondrial and cytosolic fractions, the supernatant was centrifuged at 8000 \times g for 20 min at a temperature of 4 °C. These fractions were subsequently utilized to observe the release of cytochrome *c* from the mitochondria. 1% CHAPS buffer was used to lyse mitochondrial fractions for immunoblot analysis.

2.13. Immunofluorescence

Immunofluorescence staining of 3D oncospheroids was performed as described before (Chan et al., 2021). In brief, 3D oncospheroids were collected following incubation with AlgiMatrix dissolving buffer, washed with PBS, and fixed for 10 min at room temperature in 4% PFA. Oncospheroids were permeabilized with 0.2% Triton-X for 20 min, blocked in BSA in PBS for 1 h and incubated with anti-BIM (Abcam, ab32158), anti-PUMA (Abcam, ab9645), anti-BAX (Abcam, ab216494) and anti-BAK (Abcam, ab32371) antibodies overnight at +4 °C. Following incubation with secondary antibodies (Goat Anti-Rabbit IgG (Alexa Fluor 488), ab150077; Goat Anti-Rabbit IgG (Alexa Fluor 594), ab150080; Goat Anti-Mouse IgG (Alexa Fluor 594), ab150116) for 2 h at room temperature, stained with DAPI and visualized by using EVOS FLoid Imaging Station (ThermoFisher Scientific).

2.14. Molecular docking

Molecular docking studies were conducted by Autodock Vina software (Trott and Olson, 2010). The crystal structure of Akt kinase (PDB: 3OCB) was downloaded from Protein Databank. All water molecules of protein and crystal ligand were removed, polar hydrogens and Kollman charges were added and saved into pdbqt format. A grid box was generated with dimensions of 54 \times 52 \times 52 Å (coordinate X = 5.278, Y = 0.111, Z = 4.500) with grid spacing is 0.375 Å. Exhaustiveness was set to 20. The RMSD of the docked native ligand (XM1) was found as 0.63 Å. The docking results were ranked according to the binding free energy. The interactions of compounds 5 and 8 with Akt kinase active site were evaluated with PyMOL.

2.15. Statistical analysis

Obtained data were expressed as the mean \pm standard deviation. Kruskal-Wallis ANOVA test with post-hoc Dunn's test or Mann-Whitney test were appropriately used to compare the parameters observed after the treatment of compounds to the controls. A value of $P < 0.01$ was considered statistically significant. For data analyses, IC₅₀ calculations, and graphical presentations, GraphPad Prism 7.0 software was utilized.

3. Results

3.1. Antiproliferative activities of compounds 5 and 8 in HT-29 and L929 cell lines

In this study, antiproliferative activities of the previously synthesized (Kilic-Kurt et al., 2018; Kilic-Kurt et al., 2019) compounds (1–14) were examined against MDA-MB-231, C6, and HT-29 cell lines, using the XTT assay. Initially, to identify the most active compounds, the cancer cells were exposed to target compounds at a 10 μ M constant concentration, and after treating cells for 24 h, the cell viability % (CV%) values were

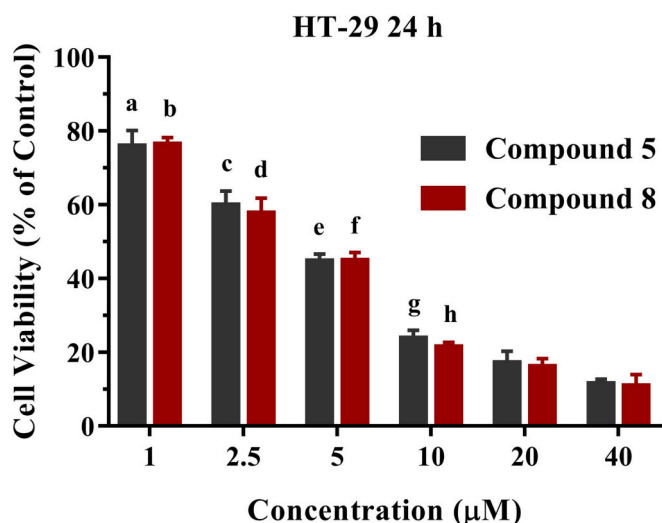


Fig. 2. Effect of compounds 5 and 8 on cell survival in HT-29 colon cancer cells. Cell viability was determined with XTT assay after compounds 5 and 8 treatment (1–40 μM) of HT-29 cell lines for 24 h. All data are presented as mean \pm SD in triplicate. The differences are identified as ** from untreated control cells ($P < 0.01$). ^{a,b} P value < 0.01 vs. 2.5, 5, 10, 20, and 40 μM concentrations; ^c P value < 0.01 vs. 5, 10, 20, and 40 μM concentrations; ^{e,f} P value < 0.01 vs. 10, 20, and 40 μM concentrations; ^{g,h} P value < 0.01 vs. 20 and 40 μM concentrations.

determined. The CV% results are summarized in Table 1. Data analysis of the CV% assay demonstrated that all the compounds generally have better antiproliferative activity against HT-29 than MDA-MB-231 and C6 cell lines. On the other hand, almost all compounds displayed moderate antiproliferative activity against MDA-MB-231 cells; however, poor cytotoxic activity was observed against C6 cells. Moreover, compounds 5 and 8 were determined as the most effective compounds against HT-29 cells with the lowest CV% of 23.82 ± 1.09 and 21.44 ± 1.71 , respectively. To determine IC_{50} values of compounds 5 and 8, HT-29 cells were also treated with 1–40 μM concentrations of these compounds for 24 h. As shown in Fig. 2, the compounds exhibited a notable inhibitory effect on the growth of HT-29 cell lines ($P < 0.01$). The IC_{50} values of compounds 5 and 8 were calculated as $4.17 \mu\text{M}$ and $2.96 \mu\text{M}$, respectively, and these IC_{50} values were also used for further assays in the rest of the studies. IC_{50} values of cisplatin as positive control were also calculated as $47.64 \mu\text{M}$, $62.14 \mu\text{M}$, $49.72 \mu\text{M}$, and $65.47 \mu\text{M}$ for MDA-MB-231, C6, HT-29, and L929 cell lines, respectively.

Furthermore, to determine the potential selective cytotoxicity of the chosen compounds towards normal and cancer cells, L929 cells were subjected to compounds 5 and 8 at 1 to 40 μM for 24 h. Compounds 5 and 8 have weak cytotoxic activity in L929 cells with IC_{50} values of 36.95 and $34.91 \mu\text{M}$, respectively (Fig. S1). Moreover, the selectivity index (SI) values of compounds 5 and 8 were calculated as 8.8 and 11.7, respectively. It should be emphasized that these compounds are significantly selective to cancer cells compared to normal cells. This may provide an additional advantage because of reduced systemic toxicity for in vivo experiments in further studies.

3.2. Treatment of compounds 5 and 8 caused cell cycle arrest and promoted apoptosis of HT-29 cells

To further evaluation of the cytotoxic activity of compounds 5 and 8, HT-29 cells were subjected to IC_{50} concentration of compounds 5 and 8 for 24 h, and the cell cycle assay was performed. As shown in Fig. 3a, treatment of HT-29 cells with compounds 5 and 8, compared to untreated cells ($23.4 \pm 1.3\%$), resulted in a significant accumulation of cell population in the G2/M phase ($P < 0.01$). The percentage of the population in the G2/M phase of compounds 5 and 8 were determined as 30.9

$\pm 1.2\%$ and $44.7 \pm 1.4\%$, respectively, suggesting that both compounds caused a significant G2/M phase arrest.

Annexin V assay was performed to evaluate the apoptotic activity of compounds 5 and 8. As shown in Fig. 3b, compounds 5 and 8 treatment significantly increased mainly late apoptosis in HT-29 cells. The percentage of cells in late apoptosis was determined as $26.60 \pm 2.89\%$ and $32.25 \pm 3.17\%$ for compound 5 and compound 8, while it was 2.23 ± 1.4 in control cells. Moreover, although the early apoptotic cell populations significantly increased in compounds 5 and 8 treated groups, the dead cell population only increased in the compound 8-treated group ($P < 0.01$).

To confirm the apoptotic effect of compounds 5 and 8, pro-apoptotic and anti-apoptotic protein expression levels were determined in compounds 5 and 8 treated and -untreated HT-29 cells. ELISA data indicated that compounds 5 and 8 treatment significantly induced Bax and cleaved caspase 3 levels ($P < 0.01$), supporting their apoptotic effects, while BCL-2 expression was not altered in response to both compounds ($P > 0.01$) (Fig. 3c-e).

In our study, caspase 3, Ki67, and p53 immunofluorescent staining results also showed that while localization of caspase 3 (Fig. 4a) and p53 (Fig. 4b) increased, the Ki67 (Fig. 4c) localization decreased compounds 5 and 8-treated groups when compared with the untreated cells (Fig. 4). These data revealed that compounds 5 and 8 treatment could trigger the apoptosis of HT-29 cells.

3.3. Effect of compounds 5 and 8 on TOS in HT-29 cells

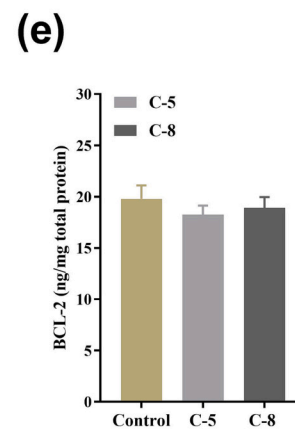
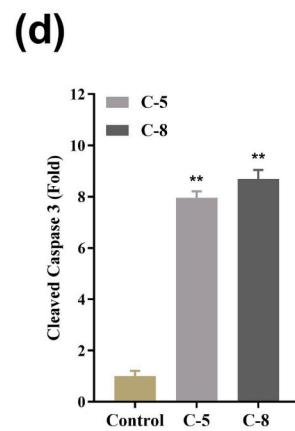
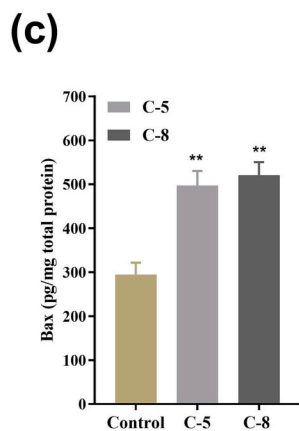
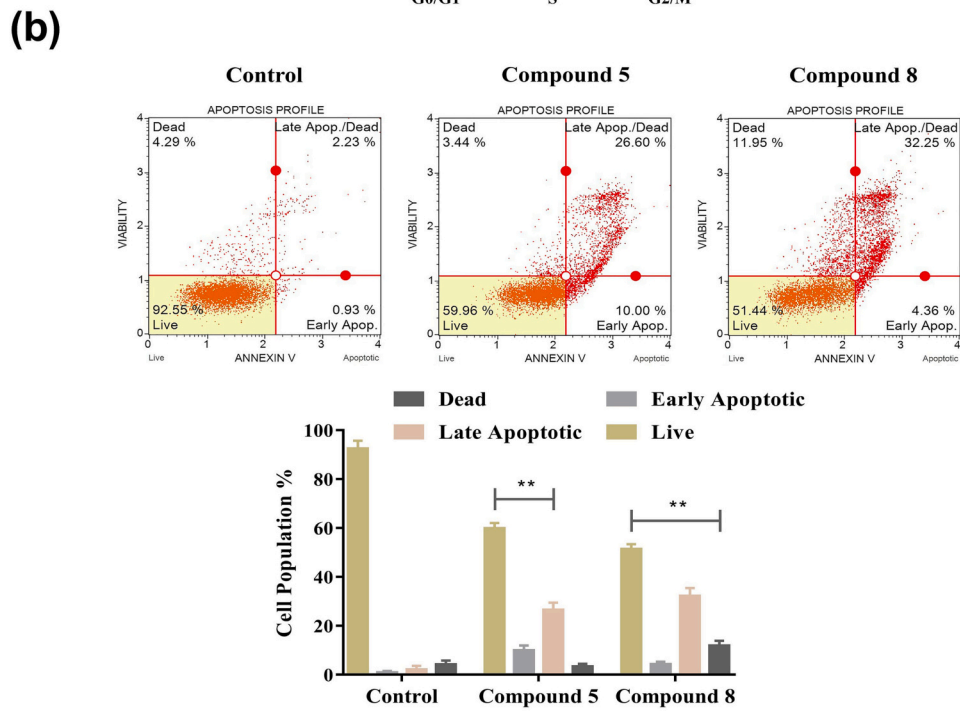
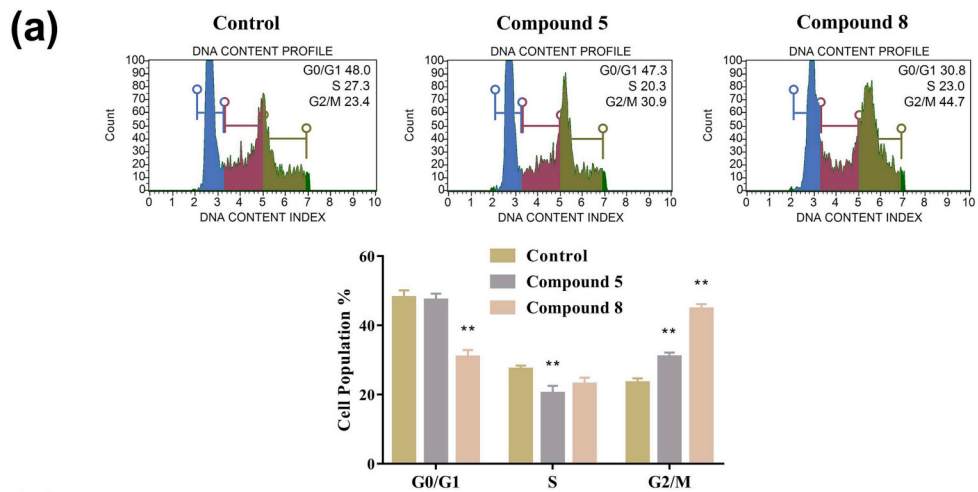
To evaluate the effect of compounds 5 and 8 on the total oxidant status (TOS) of HT-29 cells, the level of TOS was found as $5.72 \pm 0.41\%$, 8.75 ± 0.47 and 10.63 ± 0.75 in the control, compound 5- and compound 8-treated HT-29 cells, respectively ($P < 0.01$) (Fig. 5).

3.4. Effects of compound 5 and 8 on signaling pathways in HT-29 cells

To evaluate the effects of compounds 5 and 8 on signaling pathways in HT-29 cells, we evaluated the phosphorylation of Akt, ERK1/2, p38, and JNK in HT-29 cells using cell-based ELISA assays. As shown in Fig. 6A, compounds 5 and 8 led to inhibition of Akt S473 and T308 phosphorylation (Fig. 6A). Complementing this finding, exposing HT-29 cells to compounds 5 and 8 resulted in inhibition of ERK 1/2. In contrast, no alterations in JNK and p38 signaling pathways were detected (Fig. 6B). These results suggest that compounds 5 and 8 suppress two important prosurvival pathways in HT-29 cells.

Next, we tested whether treatment with compound 5 or compound 8 activates mitochondrial apoptosis in HT-29 cells. Treatment of compounds 5 and 8 led to the release of cytochrome c into the cytosol (Fig. 7A). In addition, co-treatment with irreversible pan-caspase inhibitor Q-VD-OPh significantly reduced compound 5- and compound 8-induced apoptosis in HT-29 cells, confirming the contribution of caspase-dependent mitochondrial cell death (Fig. 7A). Furthermore, we demonstrated that compound 5 or compound 8 treatment led to increased BAX, PUMA and BIM and decreased BCL-XL and MCL-1 protein levels in HT-29 cells (Fig. 7B). BCL-2 levels were also decreased upon exposure to the compounds, although less substantial compared with BCL-XL and MCL-1. Of note, we could not detect NOXA expression by using Western blot analysis in HT-29 cells even after treatment with compound 5 and compound 8. We then determined whether changes in the transcription of BCL-2 family genes contribute to the altered protein levels in HT-29 cells. qPCR data showed that PUMA and BAX expression was upregulated at mRNA level, although we did not observe a change in BIM, MCL-1, BCL-XL, or BCL-2 mRNA levels in response to treatment with compounds 5 or 8 (Figs. S2, S3). Hence, these findings suggest that the alteration of BIM, MCL-1, BCL-XL, and BCL-2 levels was a consequence of altered protein stability/turnover.

We next studied the role of BIM, PUMA, BAX, and BAK in compound 5- and compound 8-induced apoptosis in HT-29 cells. As shown in



(caption on next page)

Fig. 3. (a) Regulatory effect of compounds **5** and **8** on cell cycle progression in HT-29 cells. The cells were exposed to the compounds at IC₅₀ concentrations for 24 h, and the cell cycle distribution was evaluated using the Muse cell analyzer (Millipore). **Significantly different when compared to the cell population rate of untreated cells ($P < 0.01$) (b) Apoptotic effect of compounds **5** and **8** on HT-29 cells. The cells were treated with the IC₅₀ value of compounds **5** and **8**, and the apoptosis was determined by Muse cell analyzer (Millipore) after 24 h of treatment. While early and late apoptotic cell percentages increased significantly ($P < 0.01$) in compound **5**- and **8**-treated cells, dead cell percentage increased significantly only in compound **8**-treated cells ($P < 0.01$). Each experiment was performed at least three replicates. **Significantly different when compared to the cell population rate of untreated cells ($P < 0.01$) (c) HT-29 cells treated with compounds **5** and **8** at IC₅₀ value for 24 h, then Bax, cleaved caspase 3, and BCL-2 levels were determined using the ELISA kit. Values are mean \pm SD of three samples of the medium from wells containing HT-29 cells. **Significantly different when compared to untreated cells ($P < 0.01$)

Fig. 7C and **D**, siRNA-mediated depletion of BIM, PUMA, and BAX/BAK expression decreased apoptotic response in HT-29 cells upon exposure to compound **5** and compound **8**. Moreover, activation of caspase-3 and caspase-9 following treatment with compound **5** and compound **8** was diminished in HT-29 cells when we depleted BIM, PUMA, or BAX/BAK using RNAi (**Fig. 7E**). By contrast, reducing p53 levels in HT-29 cells did not alter apoptotic response upon treatment with compound **5** and compound **8** (**Fig. S4A, S4B**). Importantly, reducing BIM, PUMA, or BAX/BAK effectively blocked cytochrome *c* release into the cytosol, an important mitochondrial apoptosis signaling event, in response to compound **5** and compound **8** treatment (**Fig. 7F**). In line with these findings, clonogenic cell survival assays confirmed that BIM, PUMA, and BAX/BAK are required for compound **5**- or compound **8**-induced mitochondrial cell death (**Fig. S5A**).

Furthermore, reducing BIM and PUMA expression using RNAi blocked BAX and BAK activation in HT-29 cells (**Fig. S5B**). Our findings imply that both BIM and PUMA are required for the induction of mitochondrial apoptosis in HT-29 cells following treatment with compounds **5** or **8**. To demonstrate the functional contribution of BIM, PUMA, BAX, and BAK in compound **5**- or compound **8**-induced apoptosis in HT-29 cells in a model that better mimics the *in vivo* pathophysiology of tumors, we took advantage of cancer cell oncospheroids grown in 3D culture. We efficiently reduced BIM, PUMA, and BAX/BAK expression in HT-29 oncospheroids as shown by the immunofluorescence staining of oncospheroids (**Fig. 8A**). We next evaluated the effect of BIM, PUMA, or BAX/BAK depletion on compound **5**- or compound **8**-mediated cell death in HT-29 oncospheroids. Treatment of HT-29 cells with BIM, PUMA or BAX/BAK siRNAs reduced cell death response in HT-29 oncospheroids as shown by AlamarBlue assays (**Fig. 8B**). Consistent with these data, we have shown by Western blotting that depletion of BIM, PUMA or BAX/BAK was able to abrogate compound **5**- or compound **8**-induced formation of cleaved caspase-3, caspase-9, and PARP (**Fig. 8C**).

3.5. Molecular docking

Since compounds **5** and **8** inhibited the phosphorylation of Akt S473 and T308 on cell-based ELISA assays, we performed the molecular docking study to analyze the possible binding interactions of compounds with Akt kinase using Autodock vina (**Trott and Olson, 2010**). The binding modes of the compounds **5** (-11.1 kcal/mol) and **8** (-10.8 kcal/mol) in the binding site of the Akt kinase (PDB ID: 3OCB) were depicted in **Fig. 9**. Compound **5** interacted with Akt active site by forming two hydrogen bonds between NH of urea side chain and carbonyl of Glu234 and between 7-NH of pyrrolopyrimidine ring and carbonyl of Lys158. Compound **8** formed three hydrogen bonds with Glu234, Asp292, and Lys276 at Akt active site.

4. Discussion

Many studies have demonstrated the anticancer efficiency of pyrrolopyrimidine derivatives against several cancer cell lines (**Pathania and Rawal, 2018**). Among our compounds bearing methyl group at the N-7 position of pyrrolopyrimidine scaffold (**1–7**), 3-trifluoromethylphenyl urea derivative **5** exhibited the highest cytotoxic activity against HT-29 cells. Whereas the introduction of chloro (**3**) at the 4-position of 3-trifluoromethylphenylurea moiety dramatically decreased activity

(82.63%), fluoro substitution at the same position (**7**, 38.37%) was well tolerated. Replacement of 3-chloro-4-fluorophenyl moiety of compound **5** with 3-bromophenyl group (**4**, 55.46%) resulted in decreased activity in the HT-29 cells. Removing of the methyl group of compound **4** leading to **11** did not significantly improve the activity. The best active compound **8** (IC₅₀ = 2.96 μ M) was obtained by changing the 3-bromophenyl group of compound **11** with 3-trifluoromethylphenyl. Moreover, compounds **5** and **8** exhibited higher cytotoxicity than other compounds against HT-29 cells and hence these two compounds were chosen for further evaluation of the underlying mechanism of cytotoxicity.

It is well established that cell cycle arrest and apoptosis are directly linked processes, and several antiproliferative agents suppress cell proliferation by interfering with cell cycle arrest and initiating apoptosis (**Vermeulen et al., 2003**). Treatment with compounds **5** and **8** dramatically increased late apoptotic cells in HT-29 cells. It is clear that the proapoptotic protein Bax triggers the formation of a pore in the outer membrane of mitochondria and leads to its permeabilization. This also causes the release of cytochrome *c* from the mitochondria, which activates caspases including caspase 3, inhibits anti-apoptotic BCL-2 protein, and consequently causes apoptosis (**Cavalcante et al., 2019; Carneiro and El-Deiry, 2020**). On the contrary, BCL-2 protects the membrane stability, avoids the release of cytochrome *c*, and suppresses apoptosis (**Arumugam and Abdull Razis, 2018**). Caspase 3 belongs to the effector caspases family, and it serves a crucial role in apoptosis via the proteolytic cleavage of thousands of proteins. (**Arumugam and Abdull Razis, 2018; Liu et al., 2017**). We showed that increased Bax and cleaved caspase 3 expression levels by treatment of compounds **5** and **8**, supporting their apoptotic effects. p53 can induce cell death through apoptosis upon DNA damage. Ki67 antigen, however, is expressed throughout the cell cycle of proliferating cells, and many studies demonstrated that overexpression of Ki67 expression was related to worsened prognosis (**Luo et al., 2019**). We observed by immunofluorescent staining that localization of caspase 3 and p53 increased and Ki67 localization decreased suggesting the treatment of compounds **5** and **8** could trigger the apoptosis of HT-29 cells.

Oxidative stress induced by reactive oxygen species (ROS) serves an essential role in cell death, especially apoptosis through different pathways. Reactive oxygen species (ROS) are implicated in the pathogenesis of malignant tumors. In light of this information, total oxidant status (TOS) has frequently been used to assess the overall oxidation state of the body in a variety of diseases, including colon cancer (**Su et al., 2019; Wu et al., 2017**). Consistent with the relevant literature, higher cytotoxicity of compound **8** than **5** in HT-29 cells could be attributed to the meaningful increase in TOS level by compound **8**. Additionally, as elevated TOS levels contributed considerably to cell death in malignant cells, current findings supported the involvement of increased pro-oxidants in the cytotoxic and apoptotic effects of compounds **5** and **8**.

Proapoptotic activator BH3-only proteins BIM and PUMA were shown to be critical for the induction of apoptosis in various malignancies upon treatment with targeted therapies such as kinase inhibitors (**Lu et al., 2022; Tanaka et al., 2021**). Importantly, we observed that the depletion of BIM or PUMA by RNAi-mediated knockdown in HT-29 cells and oncospheroids effectively inhibited compound **5**- and compound **8**-induced apoptosis. As expected, depletion of BAX/BAK and treatment of HT-29 cells with QVD-OPh led to a similar response, further suggesting that compound **5** and compound **8** activate mitochondrial apoptotic

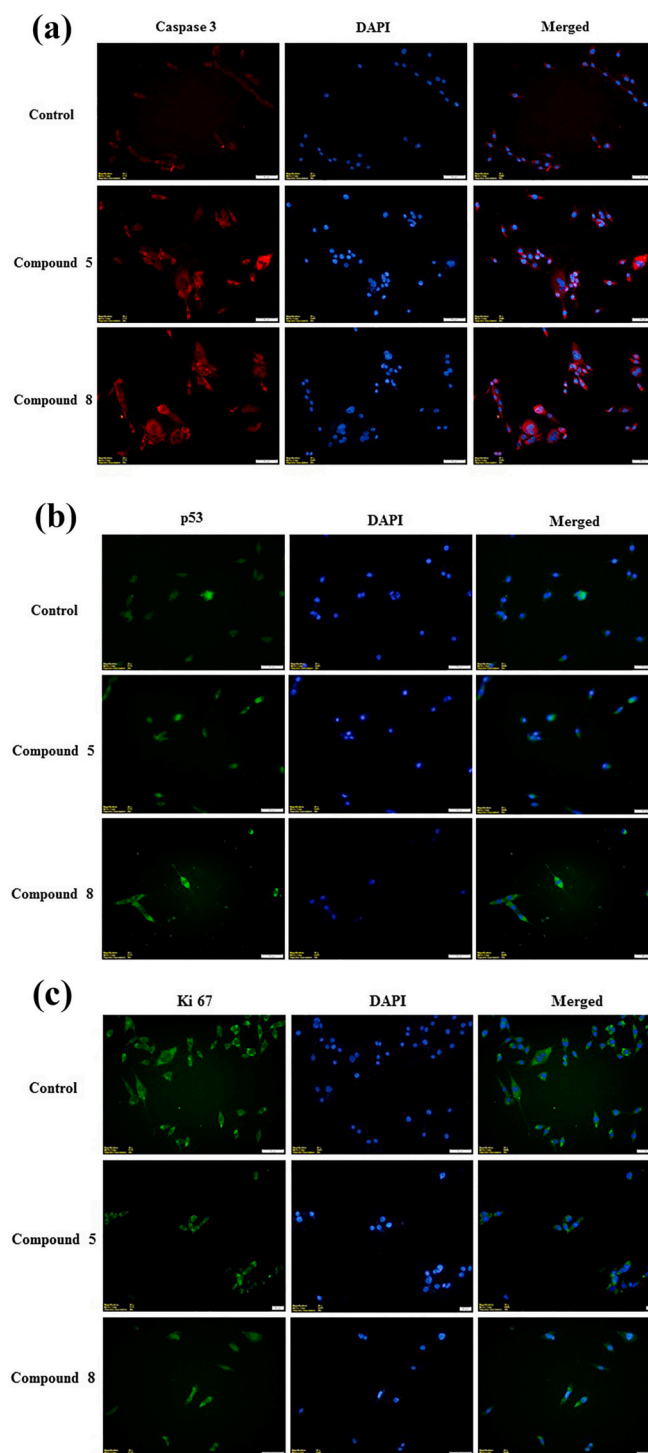


Fig. 4. (a) The localization of caspase 3 primary antibody (red) in control, compounds 5 and 8-treated HT-29 cells (Alexa Fluor® 568), and the cell nuclei are monitored in blue with DAPI staining. (b) The localization of the p53 primary antibody (green) in control, compounds 5 and 8-treated HT-29 cells (Alexa Fluor® 488), and the cell nuclei are monitored in blue with DAPI staining. (c) The localization of Ki67 primary antibody (green) in control, compounds 5 and 8-treated HT-29 cells (Alexa Fluor® 488), and the cell nuclei are monitored in blue with DAPI staining. Images obtained by caspase 3, p53, and Ki67 antibodies and DAPI staining were merged with a fluorescent microscope (Magnification X40).

pathway to induce cell death. Of note, depletion of BIM or PUMA blocked the critical proapoptotic biochemical events including cytochrome *c* release into cytosol and caspase-3/–9 activation. More importantly, we found that both BIM and PUMA are necessary for compound 5- and compound 8-induced apoptosis, suggesting the lack of functional redundancy in our experimental setting. In line with this

finding, compound 5 and compound 8 treatment resulted in decreased levels of antiapoptotic BCL-2 proteins, mainly acting on BCL-XL and MCL-1. Considering that BH3 mimetics targeting antiapoptotic BCL-2 proteins in hematological and solid cancers are being evaluated in various clinical trials (Timucin et al., 2019; Oakes et al., 2012), concomitant downregulation of antiapoptotic proteins by compound 5

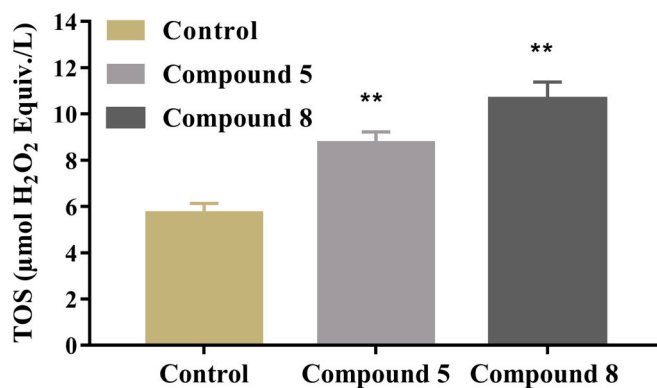


Fig. 5. Treatment of compounds 5 and 8 altered the total oxidant status (TOS) of HT-29 cells significantly. HT-29 cells were exposed to IC₅₀ concentrations of compounds 5 and 8 for 24 h and TOS were evaluated with TOS assay kit. Values are mean ± SD of three samples of the medium from wells containing HT-29 cells. **Significantly different when compared to untreated cells (*P* < 0.01).

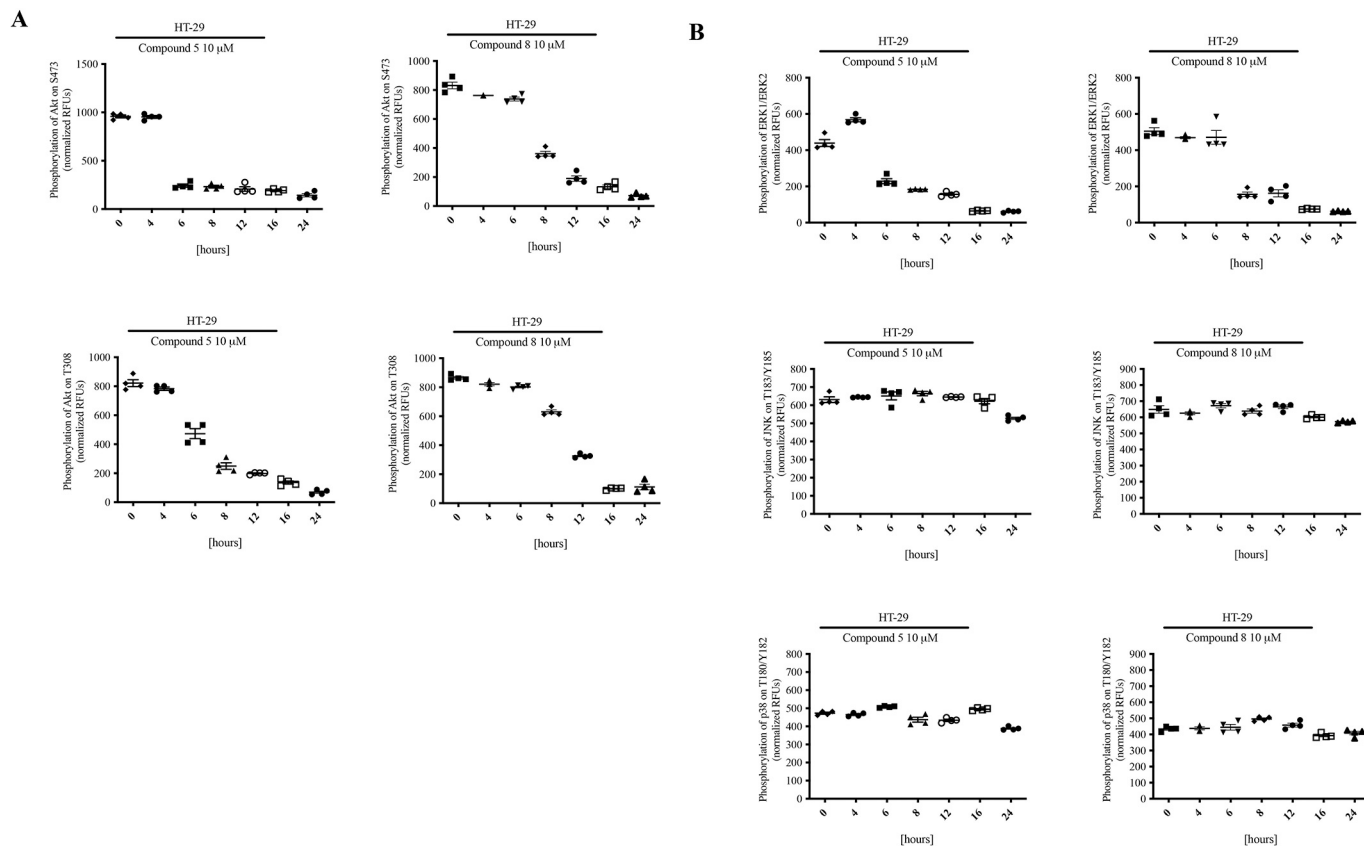


Fig. 6. Compounds 5 and 8 treatments led to inhibition of Akt and ERK1/2 activation in HT-29 cells. HT-29 cells were treated with compound 5 and compound 8 (10 µM) for 0-24 hours. Phosphorylation of (A) Akt, (B) ERK 1/2, JNK and p38 was evaluated by using cell-based ELISA assays. Data were shown as normalized fluorescence units (RFU) representing mean ± SEM of three independent experiments.

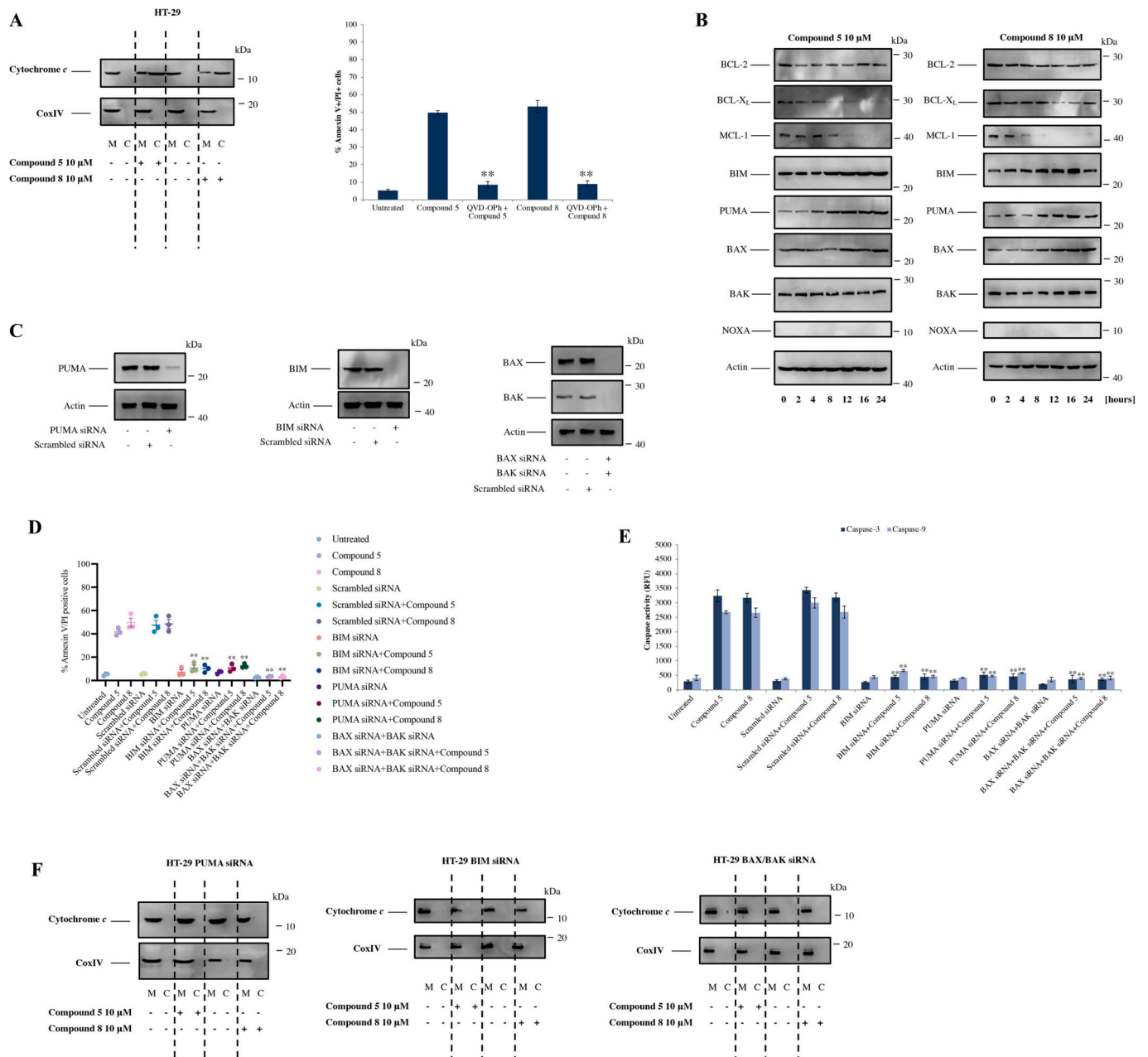


Fig. 7. BIM and PUMA are required for compound 5- and compound-8-mediated apoptotic cell death in HT-29 cells. A) HT-29 cells were treated with 10 μ M compound 5 or compound 8 for 24 hours. Cytosolic and mitochondrial fractions were blotted for cytochrome c. CoxIV was probed as loading control for mitochondrial fractions. HT-29 cells were treated with 10 μ M of compound 5 or compound 8, with or without 10 μ M broad-spectrum caspase inhibitor QVD-Oph. Apoptotic response was determined by Annexin V-FITC/PI staining. Data were shown as mean \pm SEM, $**P < 0.01$. B) HT-29 cells were treated with compound 5 or compound 8 (10 μ M). Expression of BCL-2, BCL-XL, MCL-1, BIM, PUMA, BAX, BAK and NOXA was determined by means of immunoblotting. Actin was probed as loading control. C) HT-29 cells were transfected with PUMA siRNA, BIM siRNA, BAX siRNA and BAK siRNA or scrambled siRNA for 48 hours. Expression of PUMA, BIM, BAX and BAK was detected by using immunoblotting. Actin was probed as loading control. D) Untransfected, scrambled siRNA-transfected, BIM siRNA-transfected, PUMA siRNA-transfected or BAX/BAK siRNA-transfected HT-29 cells were treated with 10 μ M of compound 5 or compound 8 for 24 h. Apoptotic response was determined by Annexin V-FITC/PI staining. Data were shown as mean \pm SEM, $**P < 0.01$. E) Untransfected, scrambled siRNA-transfected, BIM siRNA-transfected, PUMA siRNA-transfected or BAX/BAK siRNA-transfected HT-29 cells were treated with 10 μ M of compound 5 or compound 8 for 24 h. Caspase-3 and caspase-9 activities were determined by means of fluorometric caspase assays. Columns, mean relative fluorescence units (RFU) from three experimental repeats; bars, SEM; $**P < 0.01$. F) HT-29 cells were transfected with PUMA siRNA, BIM siRNA, BAX siRNA and BAK siRNA or scrambled siRNA for 48 h. Cells were treated with 10 μ M of compound 5 or compound 8 for 24 h. Cytosolic and mitochondrial fractions were blotted for cytochrome c. CoxIV was probed as loading control for mitochondrial fractions.

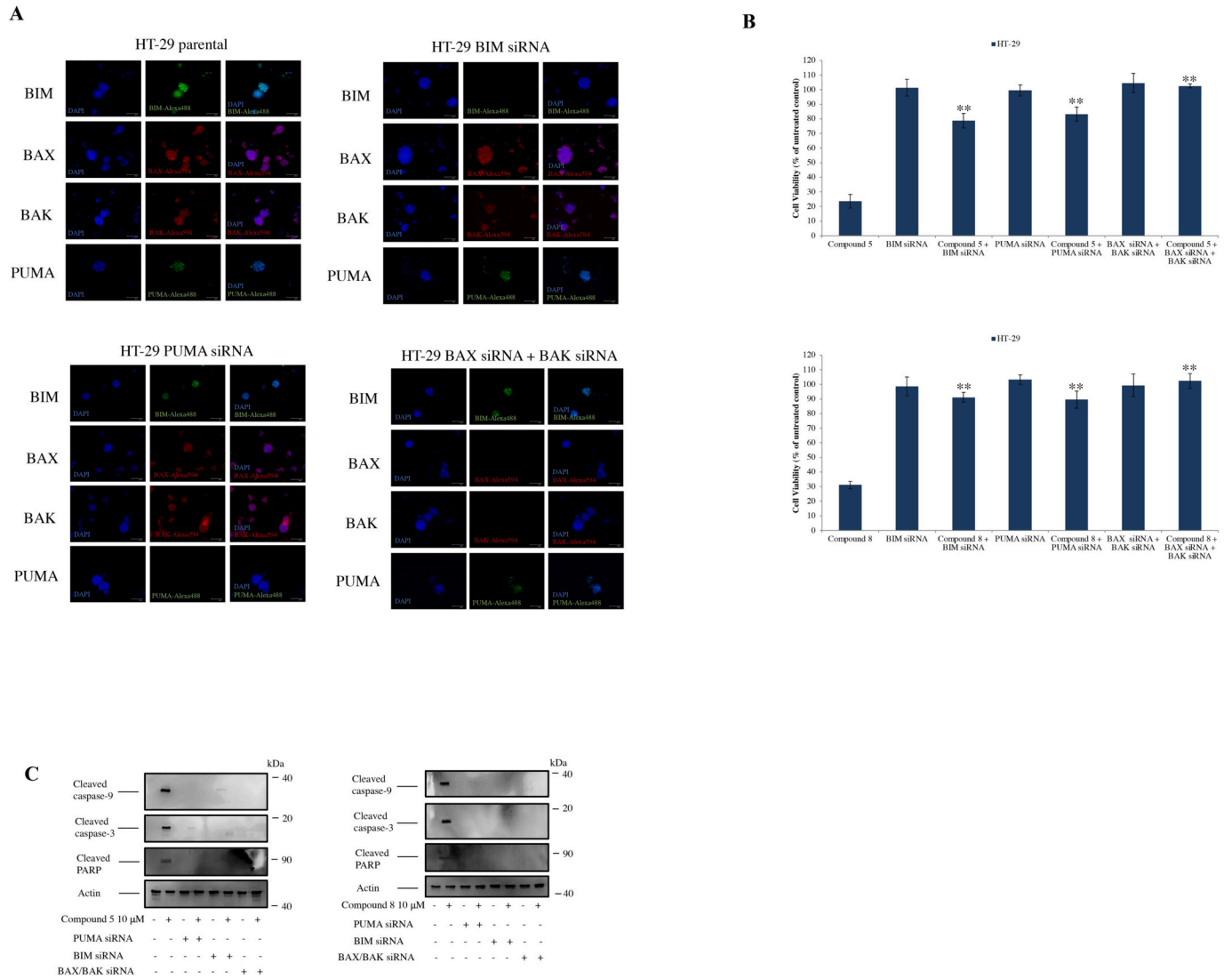


Fig. 8. Depletion of BIM, PUMA or BAX/BAK led to decreased cell death response following treatment with compound 5 or compound 8 in HT-29 oncospheroids. A) HT-29 oncospheroids were transfected with PUMA siRNA, BIM siRNA, BAX siRNA and BAK siRNA. Expression of PUMA, BIM, BAX and BAK was detected by using immunofluorescence staining. B) Cell viability was evaluated in untransfected, PUMA siRNA-transfected, BIM siRNA-transfected and BAX/BAK siRNA-transfected HT-29 oncospheroids following treatment with compound 5 (300 μM) or compound 8 (300 μM) for 24 hours by using alamarBlue assay. Results are mean values from three independent experiments (mean ± SEM, **P < 0.01). C) Activation of intrinsic apoptotic signaling in oncospheroids following treatment compound 5 (300 μM) or compound 8 (300 μM) for 24 hours was evaluated by detecting cleaved PARP, caspase-3 and caspase-9 using immunoblotting. Actin was probed as loading control.

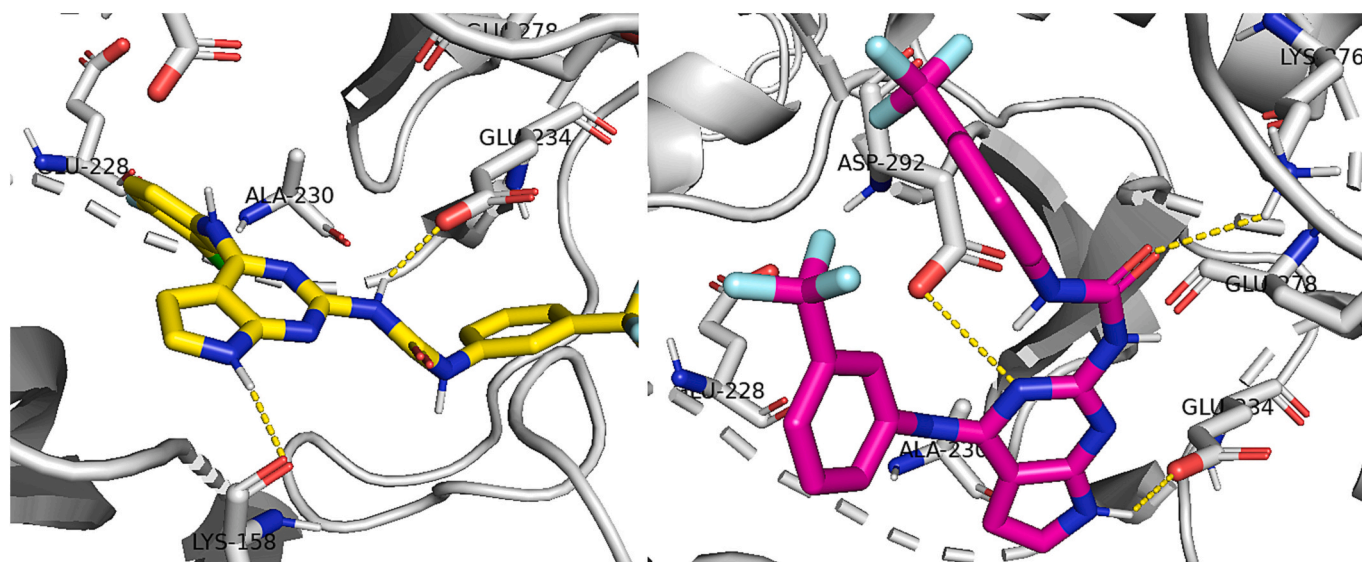


Fig. 9. Binding models of compounds **5** (left) and **8** (right) in the active site of Akt kinase. The compounds and important amino acids in the binding pockets are shown in the stick model. Hydrogen bonds are depicted as yellow dashed line.

and compound **8** indicates a potential treatment option in colon cancer cells. In addition, compound **5** and compound **8** induced apoptosis in HT-29 cells in a p53-independent manner.

5. Conclusion

In conclusion, we examined the mechanism of mitochondrial apoptosis induced by compounds **5** and **8** in HT-29 cells. These compounds caused G2/M arrest of the cell cycle, upregulated Bax, cleaved caspase 3 expressions, and altered TOS level. Moreover, while compounds **5** and **8** increased the localization of caspase 3 and p53, they decreased the Ki67 localization and finally induced apoptosis in HT-29 cells. Depletion of BIM, PUMA, and BAX/BAK by RNAi-mediated knockdown in HT-29 cells and oncospheroids and treatment of HT-29 cells with QVD-OPh resulted in decreased apoptosis in compound **5** and **8**-treated cells, indicating that compounds **5** and **8** activate the mitochondrial apoptotic pathway to cause cell death. Considering the frequency of hot-spot p53 mutations in cancer cells, including HT-29, this finding corroborates the rationale for assessing compound **5** and compound **8** as treatment options in cancers with p53 mutations. Altogether, our data demonstrated that compound **5** or compound **8** activates mitochondrial apoptosis in HT-29 colon cancer cells by upregulating both BIM and PUMA.

Supplementary data to this article can be found online at <https://doi.org/10.1016/j.tiv.2023.105757>.

Declaration of Competing Interest

The authors declare no conflict of interest.

Data availability

Data will be made available on request.

Acknowledgments

The authors would like to thank the Sivas Cumhuriyet University, School of Medicine, CUTFAM Research Center, Sivas, Turkey, for providing the necessary facilities to conduct this study.

Funding

None.

References

- Arumugam, A., Abdull Razis, A.F., 2018. Apoptosis as a mechanism of the cancer chemopreventive activity of glucosinolates: a review. *Asian Pac. J. Cancer Prev.* 19, 1439–1448. <https://doi.org/10.22034/apjcp.2018.19.6.1439>.
- Carneiro, B.A., El-Deiry, W.S., 2020. Targeting apoptosis in cancer therapy. *Nat. Rev. Clin. Oncol.* 17, 395–417. <https://doi.org/10.1038/s41571-020-0341-y>.
- Cavalcante, G.C., Schaan, A.P., Cabral, G.F., Santana-da-Silva, M.N., Pinto, P., Vidal, A. F., Ribeiro-dos-Santos, A., 2019. A Cell's fate: an overview of the molecular biology and genetics of apoptosis. *Int. J. Mol. Sci.* 20, 4133. <https://doi.org/10.3390/ijms20174133>.
- Chan, Y.H., Lee, Y.C., Hung, C.Y., Yang, P.J., Lai, P.C., Feng, S.W., 2021. Three-dimensional spheroid culture enhances multipotent differentiation and stemness capacities of human dental pulp-derived mesenchymal stem cells by modulating MAPK and NF- κ B signaling pathways. *Stem Cell Rev. Rep.* 17, 1810–1826. <https://doi.org/10.1007/s12015-021-10172-4>.
- Chen, Y.-F., Fu, L.-W., 2011. Mechanisms of acquired resistance to tyrosine kinase inhibitors. *Acta Pharm. Sin. B* 1, 197–207. <https://doi.org/10.1016/j.apsb.2011.10.007>.
- De Coen, L.M., Heugebaert, T.S.A., García, D., Stevens, C.V., 2016. Synthetic entries to and biological activity of pyrrolopyrimidines. *Chem. Rev.* 116, 80–139. <https://doi.org/10.1021/acs.chemrev.5b00483>.
- De Graaff, M.A., de Rooij, M.A., van den Akker, B.E., Gelderblom, H., Chibon, F., Coindre, J.M., Marino-Enriquez, A., Fletcher, J.A., Cleton-Jansen, A.M., Bovée, J.V., 2016. Inhibition of Bcl-2 family members sensitises soft tissue leiomyosarcomas to chemotherapy. *Br. J. Cancer* 114, 1219–1226. <https://doi.org/10.1038/bjc.2016.117>.
- Elmore, S., 2007. Apoptosis: a review of programmed cell death. *Toxicol. Pathol.* 35, 495–516. <https://doi.org/10.1080/01926230701320337>.
- Ergul, M., Bakar-Ates, F., 2019. RO3280: a novel PLK1 inhibitor, suppressed the proliferation of MCF-7 breast cancer cells through the induction of cell cycle arrest at G2/M point. *Anti Cancer Agents Med. Chem.* 19, 1846–1854. <https://doi.org/10.2174/1871520619666190618162828>.
- Fulda, S., Debatin, K.M., 2004. Targeting apoptosis pathways in cancer therapy. *Curr. Cancer Drug Targets* 4, 569–576. <https://doi.org/10.2174/156800904332763>.
- Gilson, P., Josa-Prado, F., Beauvineau, C., Naud-Martin, D., Vanwonterghem, L., Mahuteau-Betzer, F., Moreno, A., Falson, P., Lafanechère, L., Frachet, V., Coll, J.-L., Fernando Díaz, J., Hurbin, A., Busser, B., 2017. Identification of pyrrolopyrimidine derivative PP-13 as a novel microtubule-destabilizing agent with promising anticancer properties. *Sci. Rep.* 7, 10209. <https://doi.org/10.1038/s41598-017-09491-9>.
- Goldman, I.D., Zhao, R., 2002. Molecular, biochemical, and cellular pharmacology of pemetrexed. *Semin. Oncol.* 29, 3–17. <https://doi.org/10.1053/sonc.2002.37461>.
- Hurwitz, H.I., Uppal, N., Wagner, S.A., Bendell, J.C., Beck, J.T., Wade 3rd, S.M., Nemunaitis, J.J., Stella, P.J., Pipas, J.M., Wainberg, Z.A., Manges, R., Garrett, W.M., Hunter, D.S., Clark, J., Leopold, L., Sandor, V., Levy, R.S., 2015. Randomized, double-blind, phase II study of ruxolitinib or placebo in combination with capecitabine in patients with metastatic pancreatic Cancer for whom therapy with

- gemcitabine has failed. *J. Clin. Oncol.* 33, 4039–4047. <https://doi.org/10.1200/jco.2015.61.4578>.
- Indran, I.R., Tufo, G., Pervaiz, S., Brenner, C., 2011. Recent advances in apoptosis, mitochondria and drug resistance in cancer cells. *Biochim. Biophys. Acta* 1807, 735–745. <https://doi.org/10.1016/j.bbabi.2011.03.010>.
- Jeong, C.H., Joo, S.H., 2016. Downregulation of reactive oxygen species in apoptosis. *J. Cancer Prev.* 21, 13–20. <https://doi.org/10.15430/jcp.2016.21.1.13>.
- Johnson-Farley, N., Veliz, J., Bhagavathi, S., Bertino, J.R., 2015. ABT-199, a BCL2 mimetic that specifically targets Bcl-2, enhances the antitumor activity of chemotherapy, bortezomib and JQ1 in “double hit” lymphoma cells. *Leuk. Lymphoma* 56, 2146–2152. <https://doi.org/10.3109/10428194.2014.981172>.
- Karakas, B., Ozmay, Y., Basaga, H., Gul, O., Kutuk, O., 2018. Distinct apoptotic blocks mediate resistance to panHER inhibitors in HER2+ breast cancer cells. *Biochim. Biophys. Acta (BBA) – Mol. Cell Res.* 1865, 1073–1087. <https://doi.org/10.1016/j.bbamcr.2018.05.002>.
- Kilic-Kurt, Z., Bakar-Ates, F., Karakas, B., Küçük, Ö., 2018. Cytotoxic and apoptotic effects of novel Pyrrolo[2,3-d]pyrimidine derivatives containing urea moieties on cancer cell lines. *Anti Cancer Agents Med. Chem.* 18, 1303–1312. <https://doi.org/10.2174/1871520618666180605082026>.
- Kilic-Kurt, Z., Bakar-Ates, F., Aka, Y., Kutuk, O., 2019. Design, synthesis and in vitro apoptotic mechanism of novel pyrrolopyrimidine derivatives. *Bioorg. Chem.* 83, 511–519. <https://doi.org/10.1016/j.bioorg.2018.10.060>.
- Kutuk, O., Letai, A., 2008. Alteration of the mitochondrial apoptotic pathway is key to acquired paclitaxel resistance and can be reversed by ABT-737. *Cancer Res.* 68, 7985–7994. <https://doi.org/10.1158/0008-5472.Can-08-1418>.
- Liu, Y., Yin, Y., Zhang, Z., Li, C.J., Zhang, H., Zhang, D., Jiang, C., Nomie, K., Zhang, L., Wang, M.L., Zhao, G., 2017. Structural optimization elaborates novel potent Akt inhibitors with promising anticancer activity. *Eur. J. Med. Chem.* 138, 543–551. <https://doi.org/10.1016/j.ejmech.2017.06.067>.
- Lu, C., Yu, R., Zhang, C., Lin, C., Dou, Y., Wu, D., Pan, Y., Peng, T., Tang, H., Han, R., He, Y., 2022. Protective autophagy decreases lorlatinib cytotoxicity through Foxo3a-dependent inhibition of apoptosis in NSCLC. *Cell Death Dis.* 8, 221. <https://doi.org/10.1038/s41420-022-01027-z>.
- Luo, Z.-W., Zhu, M.-G., Zhang, Z.-Q., Ye, F.-J., Huang, W.-H., Luo, X.-Z., 2019. Increased expression of Ki-67 is a poor prognostic marker for colorectal cancer patients: a meta analysis. *BMC Cancer* 19, 123. <https://doi.org/10.1186/s12885-019-5324-y>.
- Mohamed, M.S., El-hameed, R.H.A., Sayed, A.I., 2017. Synthesis strategies and biological value of pyrrole and pyrrolopyrimidine. *J. Adv. Pharm. Res.* 11, 2357–2547. <https://doi.org/10.21608/APRH.2017.16155>.
- Oakes, S.R., Vaillant, F., Lim, E., Lee, L., Breslin, K., Feleppa, F., Deb, S., Ritchie, M.E., Takano, E., Ward, T., Fox, S.B., Generali, D., Smyth, G.K., Strasser, A., Huang, D.C., Visvader, J.E., Lindeman, G.J., 2012. Sensitization of BCL-2-expressing breast tumors to chemotherapy by the BCL2 mimetic ABT-737. *Proc. Natl. Acad. Sci. U. S. A.* 109, 2766–2771. <https://doi.org/10.1073/pnas.1104778108>.
- Pathania, S., Rawal, R.K., 2018. Pyrrolopyrimidines: an update on recent advancements in their medicinal attributes. *Eur. J. Med. Chem.* 157, 503–526. <https://doi.org/10.1016/j.ejmech.2018.08.023>.
- Reed, J.C., 2000. Mechanisms of apoptosis. *Am. J. Pathol.* 157, 1415–1430. [https://doi.org/10.1016/s0002-9440\(10\)64779-7](https://doi.org/10.1016/s0002-9440(10)64779-7).
- Ruiz-Vela, A., Opferman, J.T., Cheng, E.H., Korsmeyer, S.J., 2005. Proapoptotic BAX and BAK control multiple initiator caspases. *EMBO Rep.* 6, 379–385. <https://doi.org/10.1038/sj.embor.7400375>.
- Sena, P., Mancini, S., Benincasa, M., Mariani, F., Palumbo, C., Roncucci, L., 2018. Metformin induces apoptosis and alters cellular responses to oxidative stress in Ht29 colon cancer cells: preliminary findings. *Int. J. Mol. Sci.* 19.
- Simon, H.U., Haj-Yehia, A., Levi-Schaffer, F., 2000. Role of reactive oxygen species (ROS) in apoptosis induction. *Apoptosis* 5, 415–418. <https://doi.org/10.1023/a:1009616228304>.
- Singh, R., Letai, A., Sarosiek, K., 2019. Regulation of apoptosis in health and disease: the balancing act of BCL-2 family proteins. *Nat. Rev. Mol. Cell Biol.* 20, 175–193. <https://doi.org/10.1038/s41580-018-0089-8>.
- Su, L.-J., Zhang, J.-H., Gomez, H., Murugan, R., Hong, X., Xu, D., Jiang, F., Peng, Z.-Y., 2019. Reactive oxygen species-induced lipid peroxidation in apoptosis, autophagy, and ferroptosis. *Oxidative Med. Cell. Longev.* 2019, 5080843. <https://doi.org/10.1155/2019/5080843>.
- Tanaka, K., Yu, H.A., Yang, S., Han, S., Selcuklu, S.D., Kim, K., Ramani, S., Ganesan, Y.T., Moyer, A., Sinha, S., Xie, Y., Ishizawa, K., Osmanbeyoglu, H.U., Lyu, Y., Roper, N., Guha, U., Rudin, C.M., Kris, M.G., Hsieh, J.J., Cheng, E.H., 2021. Targeting Aurora B kinase prevents and overcomes resistance to EGFR inhibitors in lung cancer by enhancing BIM- and PUMA-mediated apoptosis. *Cancer Cell* 39, 1245–1261.e1246. <https://doi.org/10.1016/j.ccell.2021.07.006>.
- Temburnikar, K.W., Ross, C.R., Wilson, G.M., Balzarini, J., Cawrse, B.M., Seley-Radtke, K.L., 2015. Antiproliferative activities of halogenated pyrrolo[3,2-d]pyrimidines. *Bioorg. Med. Chem.* 23, 4354–4363. <https://doi.org/10.1016/j.bmc.2015.06.025>.
- Temel, S.G., Giray, A., Karakas, B., Gul, O., Kozanoglu, I., Celik, H., Basaga, H., Acikbas, U., Sucularli, C., Oztop, S., Aka, Y., Kutuk, O., 2020. RAB25 confers resistance to chemotherapy by altering mitochondrial apoptosis signaling in ovarian cancer cells. *Apoptosis* 25, 799–816. <https://doi.org/10.1007/s10495-020-01635-z>.
- Testa, U., Riccioni, R., 2007. Deregulation of apoptosis in acute myeloid leukemia. *Haematologica* 92, 81–94. <https://doi.org/10.3324/haematol.10279>.
- Thiriveedhi, A., Nadh, R.V., Srinivasu, N., Bobde, Y., Ghosh, B., Sekhar, K.V.G.C., 2019. Design, synthesis and anti-tumour activity of new pyrimidine-pyrrole appended triazoles. *Toxicol. in Vitro* 60, 87–96. <https://doi.org/10.1016/j.tiv.2019.05.009>.
- Timucin, A.C., Basaga, H., Kutuk, O., 2019. Selective targeting of antiapoptotic BCL-2 proteins in cancer. *Med. Res. Rev.* 39, 146–175. <https://doi.org/10.1002/med.21516>.
- Tomasini, P., Barlesi, F., Mascaux, C., Greillier, L., 2016. Pemetrexed for advanced stage nonsquamous non-small cell lung cancer: latest evidence about its extended use and outcomes. *Ther. Adv. Med. Oncol.* 8, 198–208. <https://doi.org/10.1177/1758834016644155>.
- Trott, O., Olson, A.J., 2010. AutoDock Vina: improving the speed and accuracy of docking with a new scoring function, efficient optimization, and multithreading. *J. Comput. Chem.* 31, 455–461. <https://doi.org/10.1002/jcc.21334>.
- Türe, A., Ergül, M., Ergül, M., Altun, A., Küçükgüzel, İ., 2021. Design, synthesis, and anticancer activity of novel 4-thiazolidinone-phenylaminopyrimidine hybrids. *Mol. Divers.* 25, 1025–1050. <https://doi.org/10.1007/s11030-020-10087-1>.
- Vermeulen, K., Berneman, Z.N., Van Bockstaele, D.R., 2003. Cell cycle and apoptosis. *Cell Prolif.* 36, 165–175. <https://doi.org/10.1046/j.1365-2184.2003.00267.x>.
- Wu, R., Feng, J., Yang, Y., Dai, C., Lu, A., Li, J., Liao, Y., Xiang, M., Huang, Q., Wang, D., Du, X.-B., 2017. Significance of serum total oxidant/antioxidant status in patients with colorectal cancer. *PLoS One* 12, e0170003. <https://doi.org/10.1371/journal.pone.0170003>.
- Yu, H.A., Perez, L., Chang, Q., Gao, S.P., Kris, M.G., Riely, G.J., Bromberg, J., 2017. A phase 1/2 trial of ruxolitinib and erlotinib in patients with EGFR-mutant lung adenocarcinomas with acquired resistance to erlotinib. *J. Thorac. Oncol.* 12, 102–109. <https://doi.org/10.1016/j.jtho.2016.08.140>.